J. Fluid Mech. (1974), *vol.* 66, *part* 1, *pp.* 17–33
Printed in Great Britain

Identification of turbulent wall eddies through the phase relation of the components of the fluctuating velocity gradient

By MYON KI LEE, LARRY D. ECKELMAN AND THOMAS J. HANRATTY

Department of Chemical Engineering, University of Illinois, Urbana

(Received 12 September 1973 and in revised form 22 April 1974)

Simultaneous measurements of the longitudinal (s_x) and transverse (s_z) components of the turbulent fluctuating velocity gradient at the wall of a pipe are presented for ten locations in the transverse direction. Separate measurements of s_x and of s_z are also presented for twenty locations. The s_z pattern reveals alternating positive and negative values over lengths λ of the magnitude suggested by the spacing of the streaky wall structure observed in a number of laboratories. Of particular interest is the observation of regular eddies for which the s_z pattern is accompanied by a spatial variation of s_x out of phase by about $\frac{1}{4}\lambda$. These regular eddies are associated with intermittent production of Reynolds stress and with the occurrence of large negative values of s_x which could be identified with wall bursts previously reported. The time response of the axial flow appears to influence the development of these regular eddies in that the development of an s_x pattern lags behind that of an s_z pattern. Measurements of spatial correlations of s_x and s_z with different time delays, as well as direct observations of the temporal variation of s_x and s_z patterns, support these notions.

1. Introduction

Electrochemical techniques which are the mass-transfer analogue of hot-film anemometry have been used in this laboratory to study the limiting behaviour of a turbulent field close to the wall of a pipe. Measurements of the time-averaged velocity gradient $\bar{S}$ and the two components s_x and s_z of the fluctuating velocity gradient have previously been reported for a given location on a wall (Reiss 1962; Mitchell 1965; Sirkar 1969). This paper presents the results of a study in which we measured s_x and s_z simultaneously at ten wall locations and separately at twenty wall locations. The observed instantaneous patterns of s_x and s_z provide information regarding the structure of eddies in the viscous sublayer close to the wall where viscosity is playing an important direct role in momentum transfer.

Beatty, Ferrell & Richardson (Corrsin 1956) pumped a dye solution through a pipe and observed the formation of the residual dye into streamwise filaments at the wall after flushing with water. The existence of this streaky structure was confirmed by Hama (Corrsin 1956), who injected dye through a slot in the wall. Corrsin (1956) interpreted these experiments as resulting from a predominance

of axial vorticity near the wall, which sweeps the dyed fluid into long narrow strips. Experiments by Kline & Runstadler (1959) revealed that the regions in the neighbourhood of the wall dye streaks have low velocities in the axial direction and that the average spacing between the streaks, made dimensionless with respect to the kinematic viscosity ν and the friction velocity $u^* = (\nu\bar{S})^{\frac{1}{2}}$, is $\lambda^+ \simeq 75$ for flows with zero pressure gradient. Studies of the fluctuating axial velocity gradient s_x at the wall by Reiss & Hanratty (1963) and by Mitchell & Hanratty (1966) revealed that the correlation coefficient falls to low values in distances of the order of the pipe diameter in the flow direction and in distances of the order of the thickness of the viscous wall region in the transverse direction ($z^+ = zu^*/\nu \simeq 30$). These experiments are consistent with the observed streaky structure in the immediate vicinity of the wall in that they suggest the existence of disturbances greatly elongated in the flow direction with lateral dimensions of the order of $\frac{1}{2}\lambda^+$. We call these disturbances 'large sublayer eddies'. Motion pictures of lines of hydrogen bubbles by Kline *et al.* (1967) have given more detail regarding the structure of these eddies and have allowed the measurement of instantaneous velocity patterns. The sign of the fluctuating longitudinal velocity u and the sign of the fluctuating transverse velocity w at $y^+ = uy^*/\nu = 5$ were found to alternate over distances comparable with λ^+. Kline and his co-workers attempted to find a more objective method for measuring λ^+ than counting dye streaks by taking the Fourier transform of instantaneous spatial correlations of u. On the basis of these measurements and a re-evaluation of earlier dye studies they reported $\lambda^+ \simeq 100 \pm 20$.

Another structural aspect of wall turbulence that has received considerable attention is the violent eruption of low speed fluid near the wall into the high speed outer region. Kline *et al.* (1967) identified this as starting with the lifting of a dye filament from the wall and Corino & Brodkey (1969), from motion-picture studies of the trajectories of small particles suspended in the fluid, with the eruption of fluid from the wall layer. Measurements of the velocity profile using the hydrogen-bubble technique showed, as would be expected, that the lifting of the dye filament is associated with low velocities close to the wall and an inflexion point further away from the wall. Kim, Kline & Reynolds (1971) described the bursting process as occurring in three stages in which the lifting of the low speed fluid from the wall is followed by growth of an oscillatory motion. A number of measurements of the burst frequency have been made. In contrast to the streak spacing, the burst frequency appears to scale with bulk flow parameters rather than the wall parameters u^* and ν (Kim *et al.* 1971; Rao, Narasimha & Badri Narayanan 1971). Kim *et al.* (1971) suggested that the Reynolds stress and the production of turbulence are primarily associated with the bursting phenomenon. However, visual studies by Grass (1971) and measurements by Willmarth & Tu (1967) indicate that inrushes of fluid towards the wall are also high contributors to the Reynolds stress.

A comparison of the root-mean-square value of s_x and the frequency spectrum of s_x with measurements of the streamwise fluctuating velocity u in the viscous wall region (Mitchell 1965; Fortuna 1970) supports a suggestion made by Corrsin (1956) that the viscous sublayer can be pictured as a Couette flow extending

from a fixed wall at $y^+ = 0$ to an oscillating wall at $y^+ \simeq 6$. An extrapolation of Laufer's anemometer measurements suggests, in agreement with the above model, that transverse velocities become quite small close to the wall (Hinze 1959, p. 523). However, recent measurements by Sirkar & Hanratty (1970*b*) disagree with this picture in that the magnitude of the s_z fluctuations is found to be about one third of the magnitude of the s_x fluctuations. This shows that the strong transverse velocities associated with the 'streaky structure' extend right to the wall.

The study of the motion time lines of hydrogen bubbles by Kline *et al.* (1967) represents the most significant experimental contribution to our understanding of wall eddies since it captured their structure by giving instantaneous measurements of the distribution of turbulent velocities. However, the methods for measuring these velocities are quite tedious and there is some advantage in using instrumental techniques, even though a smaller number of points can be examined. For this reason we started a study of the instantaneous velocity gradient at a large number of wall locations. The results of our initial work reported in this paper have been published in much greater detail in a Ph.D. thesis by Eckelman (1971) and an M.S. thesis by Lee (1972). Gupta, Laufer & Kaplan (1971) have used nine hot-wire probes at a distance of 0·014 in. from the wall spaced over a lateral span of 0·42 in. to measure instantaneous velocities u in the flow direction. The results reported in this paper supplement their investigation in that simultaneous measurements of the longitudinal and transverse flows are made and in that the limiting flow close to the wall is measured without any concern regarding probe interference with the flow. Of particular interest will be the phase relation between s_x and s_z. The presentation and the interpretation of our results are influenced by a model for the large sublayer eddies which Sirkar & Hanratty (1970*a*) used to interpret mass-transfer data and which Fortuna (1970) used to interpret drag-reduction measurements.

2. Models of wall eddies

One of the first attempts to model the structure of turbulence close to the wall was Townsend's (1956, p. 210) interpretation of correlation data as indicating the existence of wall-attached eddies of elongated streamwise extent. In a paper appearing in 1957 Townsend found that his simple roller eddies postulated in 1956 could not explain recent correlation measurements obtained in his laboratory (Grant 1958). He suggested instead that the constant stress layer is dominated by the irregular occurrence of nearly two-dimensional jets, directed outwards from the viscous layer and of comparatively long and indeterminate length in the direction of mean flow. The model of Bakewell & Lumley (1967) appears to be quite similar to the 1957 Townsend model in that they proposed that the wall layer is dominated by randomly located eddy pairs of elongated streamwise extent that have a much more gradual inflow towards the wall than outflow. In order to explain measurements of the fluctuating mass-transfer rate Sirkar & Hanratty (1970*a*) used a highly simplified model for the flow in the viscous sublayer which assumed that the transverse velocity associated with the large

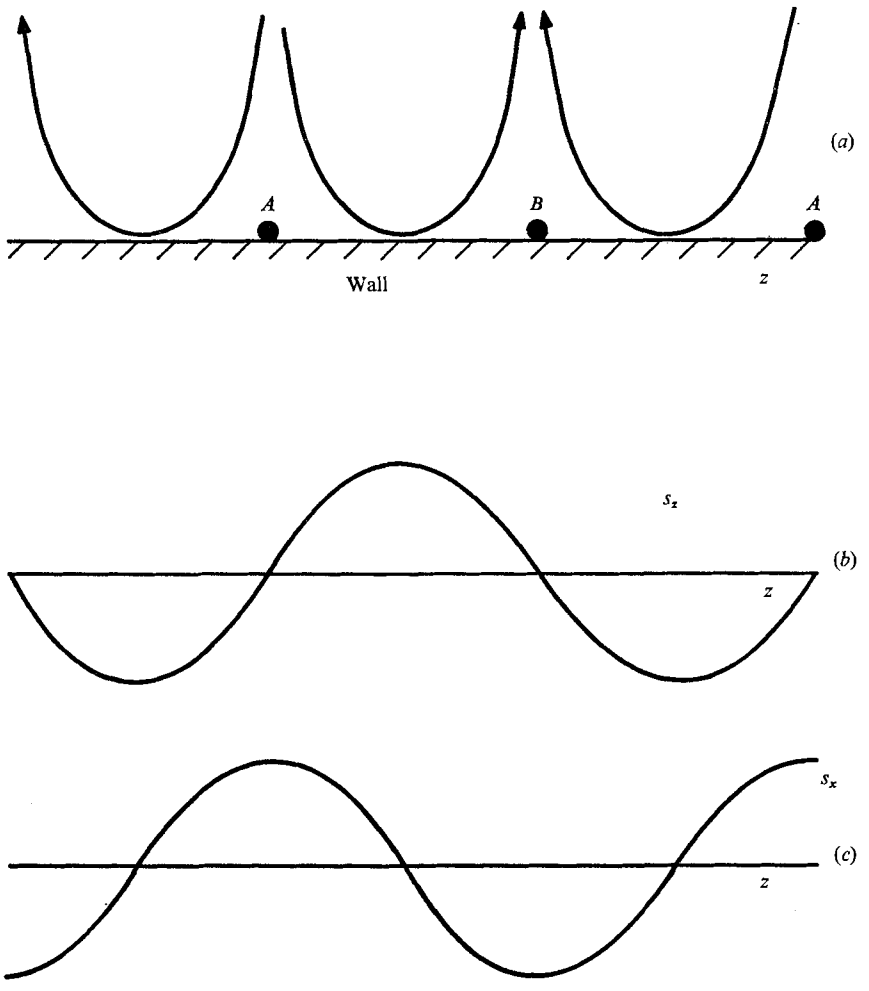

FIGURE 1. Idealized eddy pattern.

sublayer eddies is given by a function, homogeneous in the flow direction, which varies harmonically with a wavelength λ and randomly in time t:

$$w = \hat{w}(t) f(y) \sin(2\pi z/\lambda). \tag{1}$$

For the case considered by Sirkar & Hanratty $f(y) = y$ and $\hat{w}(t) = \hat{s}_z(t)$.

Fortuna (1970) has extended the model of Sirkar & Hanratty to interpret his results on momentum transfer to a wall for Newtonian and drag-reducing fluids. He assumed that the time-average velocity in the streamwise direction is largely determined by a flow-oriented large eddy structure in the immediate vicinity of the wall. Consider the secondary flow shown in figure 1(*a*) to be superimposed on the velocity in the mean flow direction. If (1) is used to describe the w velocity component, the variation of s_z at the wall will be as depicted in figure 1(*b*). The fluid moving towards the wall will carry with it x momentum associated with the outer flow. It will move along the wall, exchanging momentum

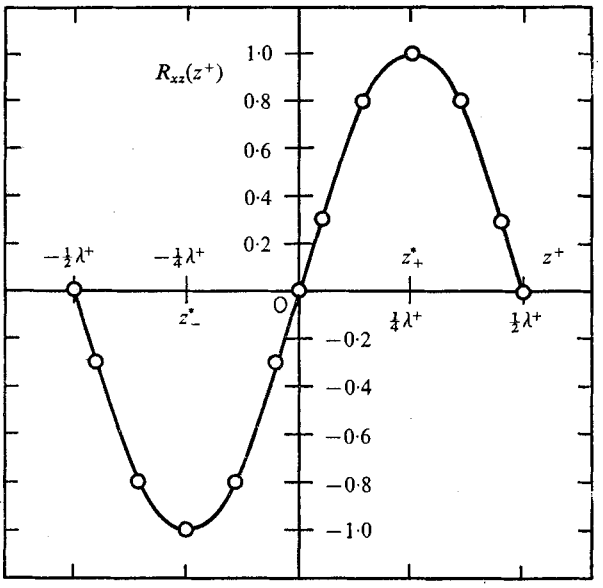

FIGURE 2. Correlation curve calculated from idealized eddy pattern.

with it, and leave the wall as momentum-deficient fluid. A corresponds to a stagnation flow and B corresponds to a low velocity streak. If a pseudo-steady-state assumption could be made the variation of s_x would be as indicated in figure 1(*c*) and there would be a definite phase relation between s_z and s_x. The location of the maximum in the correlation coefficient

$$R_{xz}(\Delta z) = \overline{s_x(z)\, s_z(z+\Delta z)}/(\overline{s_x^2})^{\frac{1}{2}}\,(\overline{s_z^2})^{\frac{1}{2}} \tag{2}$$

should be a measure of the difference in phase. In fact, if s_x were a cosine function, the simplified model depicted in figure 1 would predict that the dependence of R_{xz} on Δz is a sine function of wavelength λ, as shown in figure 2. A maximum in the correlation would then occur at a phase difference Δz between the s_x and s_z patterns of $\frac{1}{4}\lambda$.

It follows from conservation of mass and equations (7) below for the velocity field that the large sublayer eddies contribute to the Reynolds stress in the immediate vicinity of the wall according to the equation

$$-\overline{uv}/u^{*2} = \overline{\sigma_{12}}\, y^{+3}. \tag{3}$$

If $\partial s_x/\partial x$ is assumed negligible, then

$$\sigma_{12} = \tfrac{1}{2} s_x^+ \partial s_z^+/\partial z^+, \tag{4}$$

where $s_x^+ = \nu s_x/u^{*2}$ and $s_z^+ = \nu s_z/u^{*2}$. The average value

$$\langle \sigma_{12} \rangle = \frac{1}{\lambda^+}\int_0^{\lambda^+} \sigma_{12}\, dz^+ \tag{5}$$

of σ_{12} over the surface is a maximum when the phase difference between the s_x and s_z patterns equals $\frac{1}{4}\lambda^+$.

3. Description of experiments

The experiments were conducted in our flow loop containing a pipe 7·615 in. in diameter (Sirkar 1969). The electrochemical technique used to measure s_x and s_z is based on the following redox reaction of ferri- and ferrocyanide in an aqueous solution of 0·01 N potassium ferri- and ferrocyanide in a supporting electrolyte of 1 N sodium hydroxide:

$$\mathrm{Fe(CN)_6^{-3}} + e^- \rightarrow \mathrm{Fe(CN)_6^{-4}} \quad \text{at the cathode,}$$

$$\mathrm{Fe(CN)_6^{-4}} \rightarrow \mathrm{Fe(CN)_6^{-3}} + e^- \quad \text{at the anode.}$$

The cathode, a small platinum electrode mounted flush with the wall of the pipe, has a much smaller area than the anode so that the current is controlled by the events at the cathode. The applied voltage is so large that the concentration of ferricyanide ions at the cathode is essentially zero and the electric current is diffusion controlled.

The mass-transfer coefficient K describing the rate of transfer of the ferricyanide ions to the cathode is related to the electric current I by

$$K = I/FA_eC_b, \tag{6}$$

where F = Faraday's constant, A_e = electrode area and C_b = bulk average concentration.

Because of the thinness of the concentration boundary layer ($y^+ < 0{\cdot}5$), the fluid velocities in this region may be represented as

$$\bar{U} = \bar{S}_x y, \quad u = s_x y, \quad w = s_z y, \tag{7}$$

so that the mass-transfer coefficient can be related to the flow field by a solution of the mass balance equation:

$$K = \alpha |S/L|^{\frac{1}{3}}, \tag{8}$$

where

$$|S| = [(\bar{S}_x + s_x)^2 + s_z^2]^{\frac{1}{2}}, \tag{9}$$

L is the length of the electrode and α is a proportionality constant. For a pair of electrodes slanted at angles $\pm\phi$ to the direction of mean flow, Sirkar & Hanratty (1969) have shown after some approximations that

$$\frac{k_-}{\bar{K}} \simeq \frac{2}{3}\frac{s_z}{\bar{S}_x}\left[\frac{\cot\phi - (2L/5W)\cot^2\phi}{1 + (L/5W)\cot\phi}\right] \tag{10}$$

and

$$\frac{k^+}{\bar{K}} \simeq \frac{2}{3}\frac{s_x}{\bar{S}_x}, \tag{11}$$

where $k_- = K_1 - K_2$, $k_+ = (K_1 - \bar{K}) + (K_2 - \bar{K})$ and W is the width of the electrode. Thus, the s_x and s_z fluctuations may be simultaneously measured with the electrode pair by adding and subtracting the two signals respectively. Ten electrode pairs in the transverse direction were selected for simultaneous measurements of s_x and s_z and twenty for separate s_x or s_z measurements. The data were either fed into an IBM 1800 computer or were recorded on tape. Krohn–Hite 330A low frequency band-pass filters were used to cut off high frequency noise when making correlation measurements and fourteen filter circuits of the type shown in figure 3 were used to study the effect of filtering on the eddy structure.

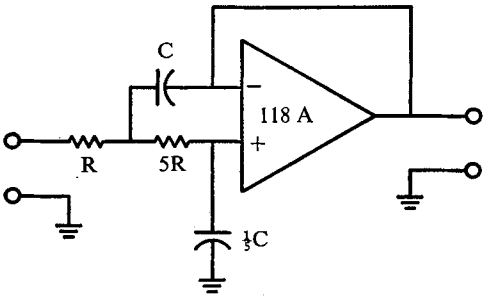

FIGURE 3. Filtering circuit.

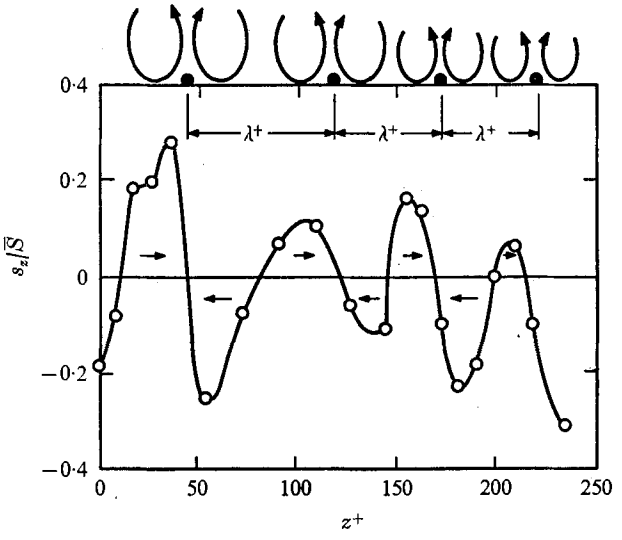

FIGURE 4. Determination of eddy structure from instantaneous velocity measurements. $Re = 35900$.

The spatial correlation measurements were carried out on a Boonshaft & Fuchs Inc. Model 711CL analyser, and correlation measurements with time delay on the Saicor Model SAI-43A probability/correlator. Other analyses of the instantaneous eddy pattern were made from data recorded in an IBM 1800 computer. In the calculation of σ_{12} a linear relationship was assumed to estimate the average values of s_x and $\partial s_z/\partial z$ half-way between two adjacent stations. Since the non-dimensional distance is 9·4, the spatial resolution of $\partial s_z/\partial z$ is rather poor.

4. Experimental results for patterns of s_x and s_z

Simultaneous measurements of s_z at twenty wall locations are shown in figure 4. These data suggest the eddy structure shown above the figure. If dye streaks at the wall are associated with updrafts then the indicated dimensionless streak spacings λ^+ are obtained.

We have analysed a large number of these eddy patterns to determine the distribution functions describing the dimensionless distance $l^+ = lu^*/\nu$ between

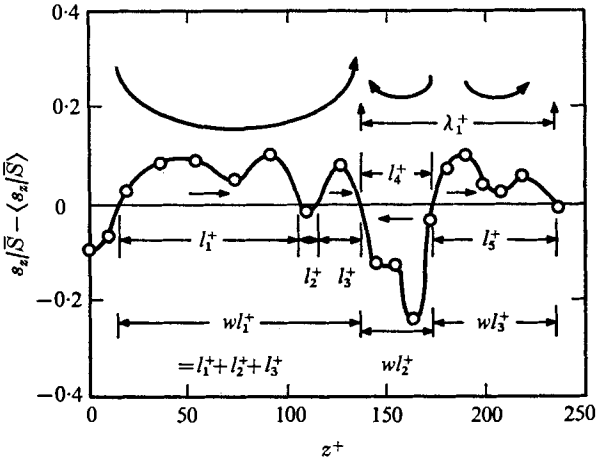

FIGURE 5. Selection of eddy size. Re = 35900. (Angular brackets signify an average in the z direction.)

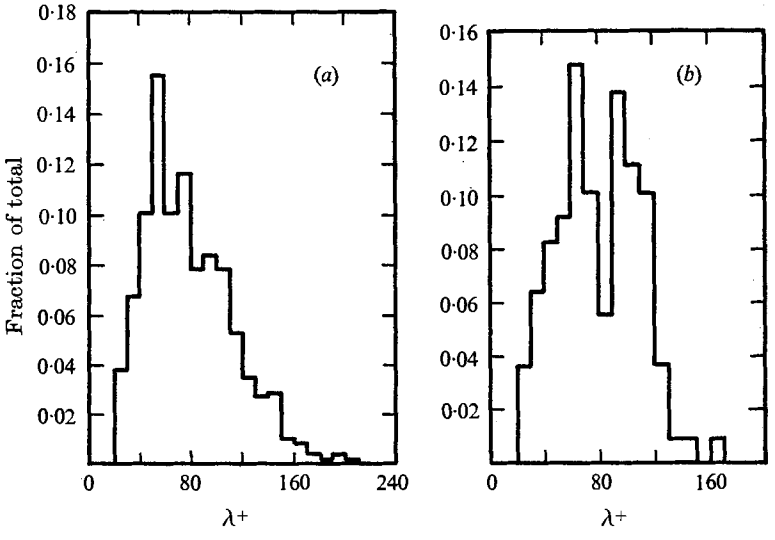

FIGURE 6. Probability distributions of wavelengths. (*a*) Transverse velocity; Re = 35900. (*b*) Axial velocity; Re = 16100.

zero crossings and the dimensionless distance λ^+ between updrafts of large sublayer eddies. An examination of these patterns suggests that values of $l^+ < 10$ should be ignored in order to avoid unrealistic situations in which a very small eddy would be paired with a large one. A detailed account of the reasoning behind this selection process is given in Eckelman (1971). The consequences of ignoring $l^+ < 10$ are shown in figure 5, where a direct measurement of the distance between zero crossings gives five values of l^+. The neglect of l_2^+ reduces these to three: $wl_1^+ = l_1^+ + l_2^+ + l_3^+$, $wl_2^+ = l_4^+$ and $wl_3^+ = l_5^+$.

A distribution function of λ^+ calculated from s_z patterns at a Reynolds number

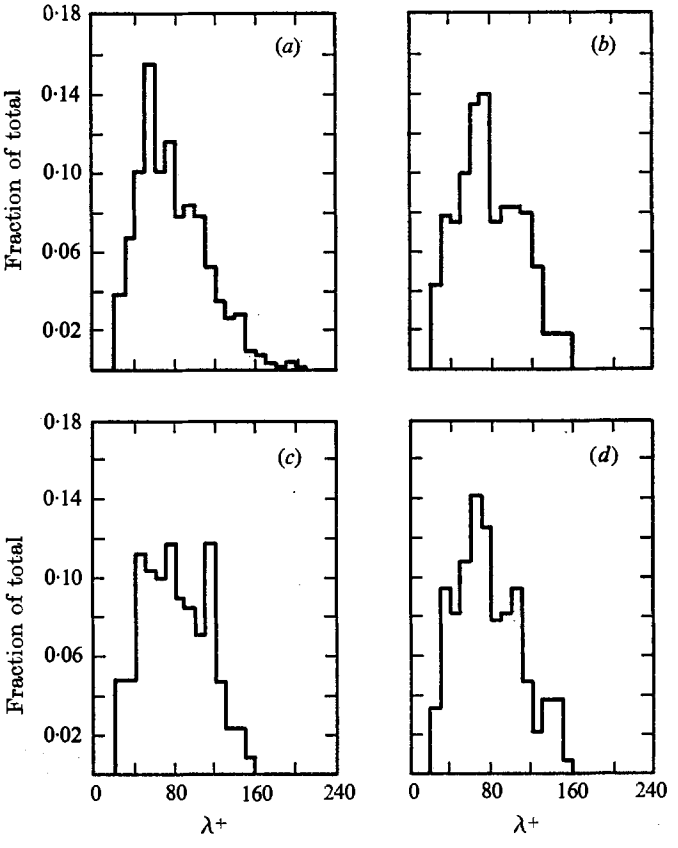

FIGURE 7. Probability distributions of wavelengths of transverse velocity. Re = 35900. (*a*) Full energy. (*b*) 89 % of energy. (*c*) 62 % of energy. (*d*) 33 % of energy.

of 35900 is shown in figure 6(*a*). A similar analysis of s_x patterns at a Reynolds number of 16100 gives the result shown in figure 6(*b*). The average value of λ^+ is 75 for both the s_x and s_z patterns. As indicated in table 1, the value 75 is close enough to values reported by other authors to suggest that the pattern of variation of wall velocity gradients corresponds to the streaky wall structure discussed in the literature.

In order to determine whether the magnitude of the wavelength of the large sublayer eddies is related to their frequency we filtered different amounts of the high frequency energy from the transverse velocity signals. Cut-off frequencies $n_c^+ = n_c \nu / u^{*2}$ of $1{\cdot}86 \times 10^{-2}$, $9{\cdot}34 \times 10^{-3}$ and $4{\cdot}67 \times 10^{-3}$ were investigated. These corresponded to passing 89, 62 and 33 % of the energy. This filtering reduced the amplitude but had only a minor effect on the wavelength of the eddy patterns. This can be seen by the wavelength distribution functions shown in figure 7. These results support the notion presented in (1) that the velocity variation in the large sublayer eddies can be modelled as the product of a function of a space and a function of time.

Spatial correlation coefficients R_{zz} of the transverse component of the velocity

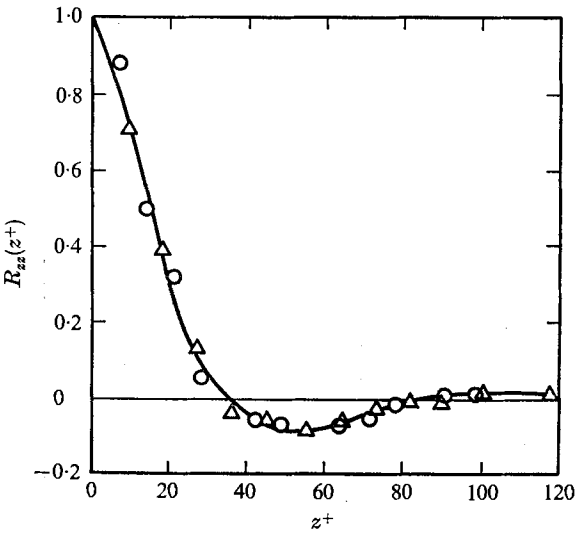

FIGURE 8. Spatial correlation of transverse velocity. ○, Re = 26900; △, Re = 35900.

Source	Re	$\lambda^+ = \lambda u^*/\nu$	Remarks
This work	34700	106	Correlation measurement
This work	37200	105	Correlation measurement
This work	40900	107	Correlation measurement
Kim *et al.* (1971)	2000	100 ± 20	Dye and H_2 bubbles, water
Clark (1968)	30000	100	H_2 bubbles, water
Coantic (1967)	2500	$110 \sim 130$	Hot-wire correlation, air
Bakewell & Lumley (1967)	~ 1877	~ 100	Hot-wire correlation, glycerine and water
Gupta *et al.* (1971)	$2000 \sim 6500$	~ 95	Air, multiple hot-wire correlation

TABLE 1. Average wavelength of a large sublayer eddy structure.

gradient are shown in figure 8. Negative values are obtained at large values of z^+ as would be suggested by a model of counter-rotating eddies attached to the wall. However the negative peak is not very large because the eddies have a distribution of wavelengths.

5. Experimental results on simultaneous measurements of s_x and s_z

The simultaneous measurements of s_x and s_z at ten wall locations gave more insight into the eddy structure than do the separate measurements of s_x and s_z just discussed. One of the striking features of these patterns is that on many occasions the phase difference between s_x and s_z is as depicted in figures 1 (*b*) and (*c*) for the idealized eddy model. Typical examples of these 'regular' eddy patterns are shown in figure 9.

In order to obtain more quantitative evidence for their existence we measured the spatial correlation between the longitudinal and transverse components of

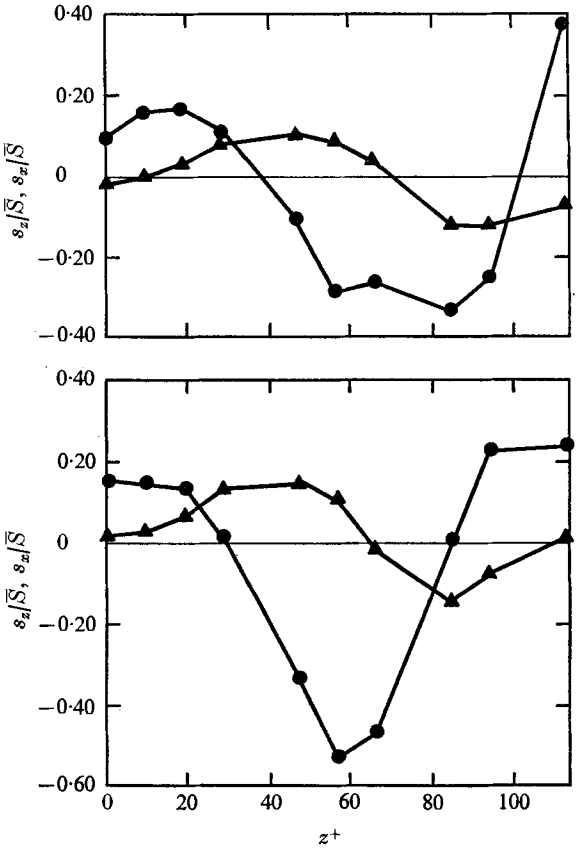

FIGURE 9. Profiles of axial and transverse velocities. Re = 37200. ▲, $s_z/\overline{S}$; ●, $s_x/\overline{S}$.

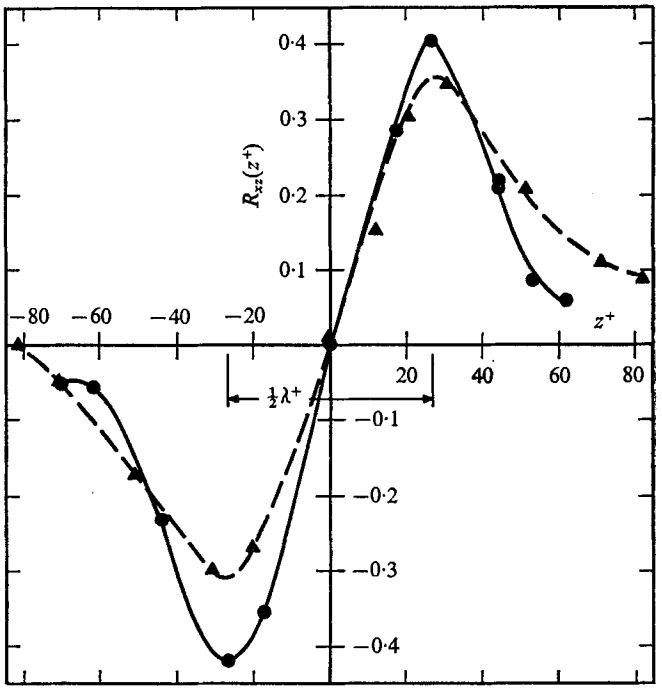

FIGUER 10. Determination of average wavelength of eddies from correlation of axial and transverse velocities. ●, Re = 34700; ▲, Re = 40900.

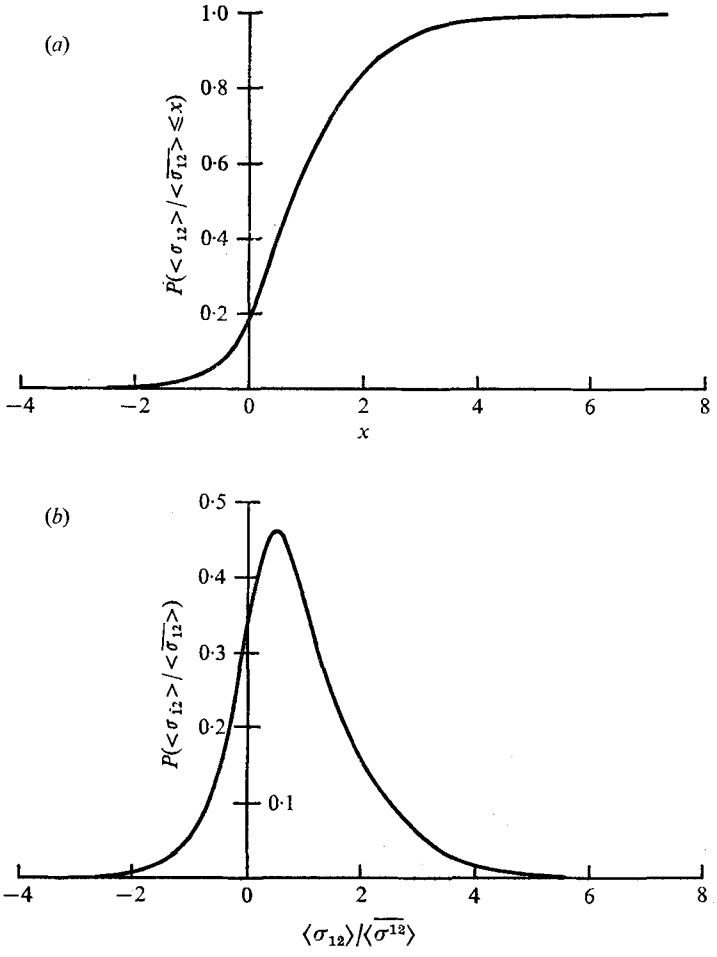

FIGURE 11. (*a*) Probability distribution of $\langle\sigma_{12}\rangle$ and (*b*) probability density function of $\langle\sigma_{12}\rangle$.

the velocity gradient. The correlation coefficients shown in figure 10 reveal a positive peak at $z_+^* \simeq 27$ and a negative peak at $z_-^* \simeq -26$. From figure 2 we estimate the wavelength of the wall eddies to be

$$\lambda^+ = 2(z_+^* - z_-^*). \tag{12}$$

Values of λ^+ calculated using (12) are compared with estimates in the literature in table 1. Good agreement is noted.

In order to obtain a numerical measure of how often these idealized eddy patterns are observed we calculated values of the Reynolds stress function $\langle\sigma_{12}\rangle$ defined by (5). The probability distribution and the probability density of $\langle\sigma_{12}\rangle$ are shown in figures 11 (*a*) and (*b*). From figure 11 (*b*) we can determine a value of C_R for which

$$\int_{-\infty}^{C_R} P(q)\,dq = 0, \quad q = \langle\sigma_{12}\rangle/\langle\overline{\sigma_{12}}\rangle.$$

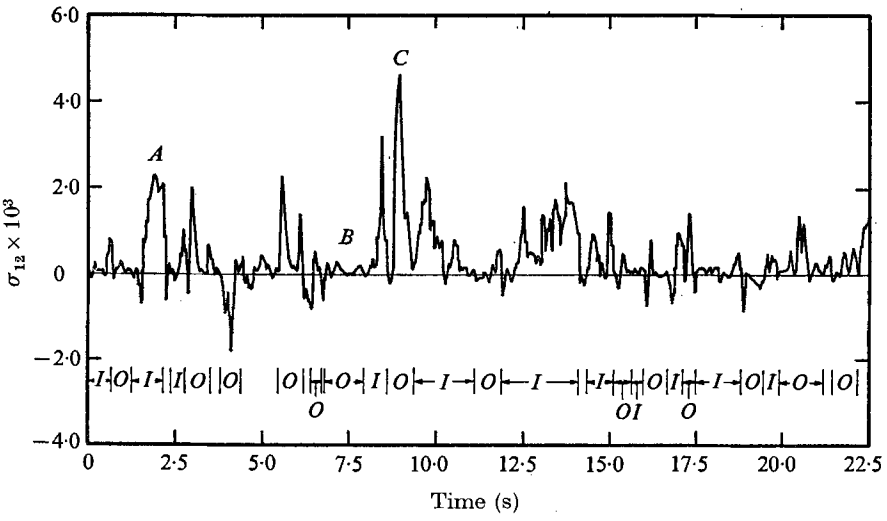

FIGURE 12. Variation of Reynolds stress function with time at $z^+ = 61$. *I*, inflow; *O*, outflow.

We have arbitrarily defined 'regular' eddy patterns to exist for $\langle\sigma_{12}\rangle/\langle\overline{\sigma_{12}}\rangle$ greater than C_R. From this criterion we determine that they exist about 59 % of of the time.

6. Production of Reynolds stress by large eddies

Measurements of the time variation of the local value of the Reynolds stress function σ_{12} are shown in figure 12. It is of interest to note that this is intermittent even though s_x and s_z are not intermittent. The same type of behaviour is exhibited by the Reynolds stress measurements of Eckelmann (1970) and of Willmarth & Lu (1972) in a wall layer.

In figure 12 we have denoted inflows by the symbol *I* and outflows by *O*. In figures 13(*a*), (*b*) and (*c*) are plotted eddy patterns associated with values of σ_{12} indicated in figure 12. We note that large values of σ_{12} are associated with eddy patterns of the type shown in figure 1. We find that outflows with large peak values of σ_{12} usually have large negative values of s_x and we therefore suggest that these could be associated with the bursting phenomenon reported in the literature.

7. Temporal phase lag of s_x

We have conditionally examined a large number of measurements of the type shown in figure 13 with the intent of discovering conditions under which idealized eddy patterns are established. As yet, no definite conclusions have been reached. However, we do find that the time response of the velocity field in the x direction is playing an important role. This is evidenced by the tendency of changes in the s_x pattern to lag behind sudden changes in the s_z pattern.

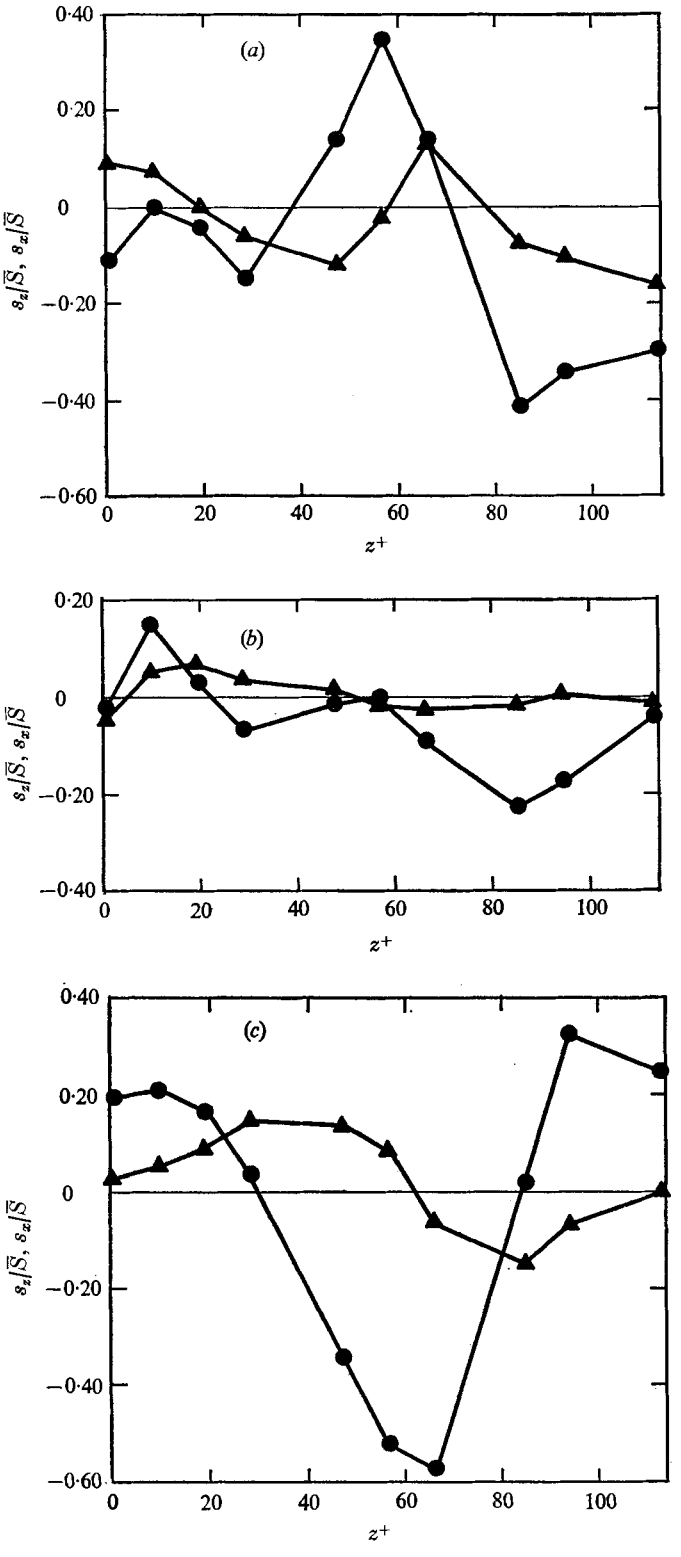

FIGURE 13. Eddy patterns (*a*) for an inflow (point *A*), (*b*) for a non-bursting period (point *B*) and (*c*) during bursting (point *C*). ▲, $s_z/\overline{S}$; ●, $s_x/\overline{S}$.

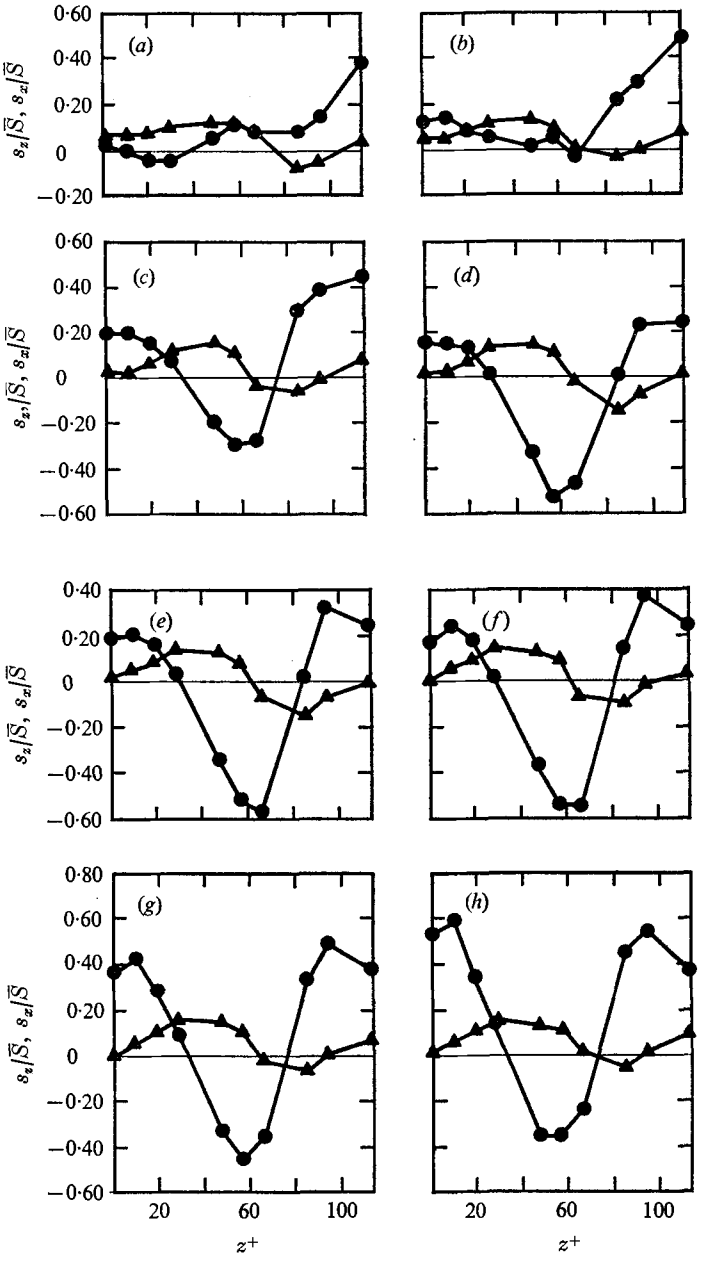

FIGURES 14(*a*)–(*h*). For legend see next page.

Figure 14 shows the sequence of events quite often observed to lead to the development of a 'burst', as defined in the previous section. Initially, there is a change in the s_z pattern, which shows a counter-rotating eddy pair. The s_x pattern does not respond immediately but lags behind. Eventually, when a stable s_z pattern is established, the s_x pattern adjusts its phase so that a regular eddy

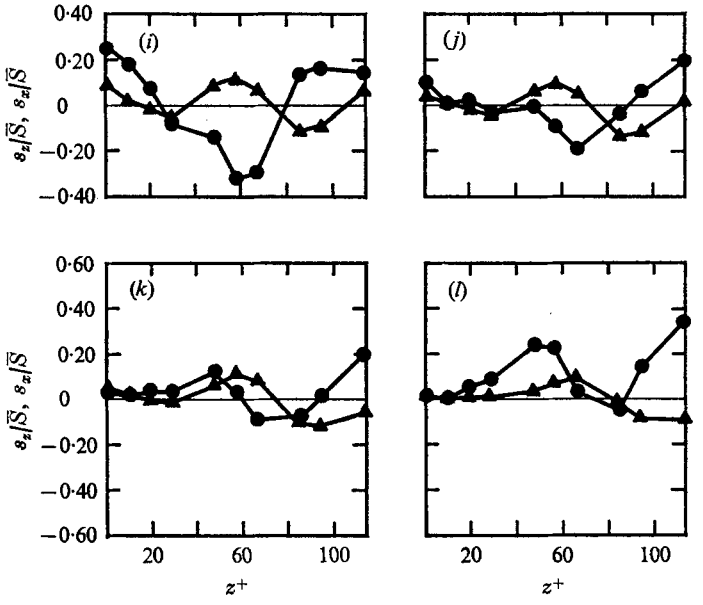

FIGURE Eddy patterns during bursting period. ▲, $s_z/\bar{S}$; ●, $s_x/\bar{S}$. (*a*) Time T = 8·696 s. (*b*) T = 8·750 s. (*c*) T = 8·804 s. (*d*) T = 8·857 s. (*e*) T = 8·911 s. (*f*) T = 8·965 s. (*g*) T = 9·019 s. (*h*) T = 9·072 s. (*i*) T = 9·233 s. (*j*) T = 9·287 s. (*k*) T = 9·340 s. (*l*) T = 9·394 s.

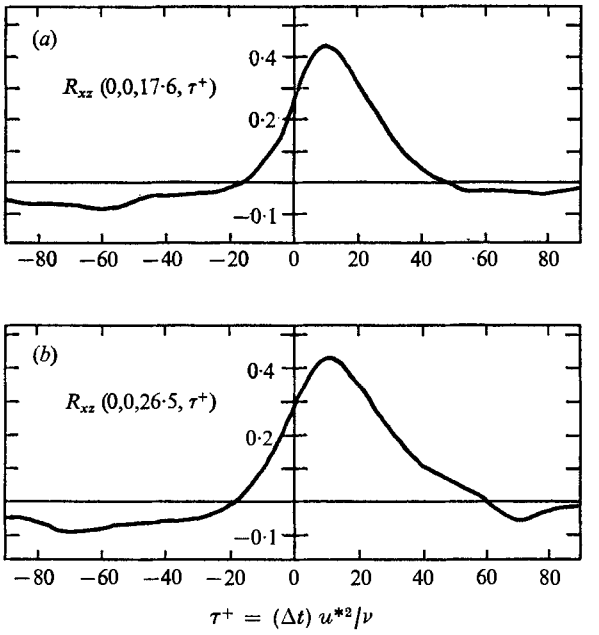

FIGURE 15. Correlation between axial and transverse velocity with time delay. Re = 34700. (*a*) Δz^+ = 17·6. (*b*) Δz^+ = 26·5.

structure is established. If the s_z pattern remains reasonably steady the amplitude of the variation of s_x increases, so that extremely large negative values of s_x develop.

These results support the notion that the s_x pattern is largely controlled by the transverse velocity field. They also suggest that correlation measurements of s_x and s_z in which s_z is delayed temporally should reveal a larger peak than is shown in figure 10. This suggestion is confirmed by the data in figure 15, which shows correlations of s_x and s_z for fixed values of the lateral spacing Δz and with different amounts of time delay for s_z. It is noted that a maximum in the correlation with $\Delta z \simeq \frac{1}{4}\lambda$ is obtained for a dimensionless delay time $\tau^+ \simeq 10{\cdot}5$. Similar correlation measurements with s_x or s_z alone show a peak at $\tau^+ = 0$. We conclude that the peak observed in figure 15 is caused by the tendency of changes in the s_x pattern to lag behind changes in the s_z pattern.

This work has been supported by the National Science Foundation under Grants NSF GK-40745 and NSF GK-2813X.

REFERENCES

BAKEWELL, H. P. & LUMLEY, J. L. 1967 *Phys. Fluids*, **10**, 1880.

CLARK, J. A. 1968 *J. Basic Engng, Trans. A.S.M.E.* **90**, 455.

COANTIC, M. 1967 *Proc. 4th Euromech. Colloq., Southampton.*

CORINO, E. R. & BRODKEY, R. S. 1969 *J. Fluid Mech.* **37**, 1.

CORRSIN, S. 1956 *Symp. on Naval Hydrodyn.*, p. 373.

ECKELMAN, L. D. 1971 Ph.D. thesis, University of Illinois.

ECKELMANN, H. 1970 *Mitteilungen MPI für Strömungsforschung und der AVA, Göttingen*, no. 48.

FORTUNA, G. 1970 Ph.D. thesis, University of Illinois.

GRANT, H. L. 1958 *J. Fluid Mech.* **4**, 149.

GRASS, A. J. 1971 *J. Fluid Mech.* **50**, 233.

GUPTA, A. K., LAUFER, J. & KAPLAN, R. E. 1971 *J. Fluid Mech.* **50**, 493.

HINZE, J. O. 1959 *Turbulence*, p. 523. McGraw-Hill.

KIM, H. T., KLINE, S. J. & REYNOLDS, W. C. 1971 *J. Fluid Mech.* **50**, 133.

KLINE, S. J., REYNOLDS, W. C., SCHRAUB, F. A. & RUNSTADLER, P. W. 1967 *J. Fluid Mech.* **30**, 741.

KLINE, S. J. & RUNSTADLER, P. W. 1959 *J. Appl. Mech., Trans. A.S.M.E.* **26**, 166.

LEE, M. K. 1972 M.S. thesis, University of Illinois.

MITCHELL, J. E. 1965 Ph.D. thesis, University of Illinois.

MITCHELL, J. E. & HANRATTY, T. J. 1966 *J. Fluid Mech.* **26**, 199.

RAO, K. N., NARASIMHA, R. & BADRI NARAYANAN, M. A. 1971 *J. Fluid Mech.* **48**, 339.

REISS, L. P. 1962 Ph.D. thesis, University of Illinois.

REISS, L. P. & HANRATTY, T. J. 1963 *A.I.Ch.E. J.* **9**, 154.

SIRKAR, K. K. 1969 Ph.D. thesis, University of Illinois.

SIRKAR, K. K. & HANRATTY, T. J. 1969 *Indust. & Engng Chem. Fund.* **8**, 189.

SIRKAR, K. K. & HANRATTY, T. J. 1970*a* *J. Fluid Mech.* **44**, 589.

SIRKAR, K. K. & HANRATTY, T. J. 1970*b* *J. Fluid Mech.* **44**, 605.

TOWNSEND, A. A. 1956 *The Structure of Turbulent Shear Flow.* Cambridge University Press.

TOWNSEND, A. A. 1957 *Symp. Int. Union of Theor. & Appl. Mech.*, p. 1. Springer.

WILLMARTH, W. W. & LU, S. S. 1972 *J. Fluid Mech.* **55**, 65.

WILLMARTH, W. W. & TU, B. J. 1967 *Phys. Fluids*, **9** (suppl.), 134.